APPLIED PHYSICS LETTERS 113, 062105 (2018)

Activation of buried p-GaN in MOCVD-regrown vertical structures

Wenshen Li,[1,a)] Kazuki Nomoto,[1] Kevin Lee,[1] S. M. Islam,[1] Zongyang Hu,[1] Mingda Zhu,[1] Xiang Gao,[2] Jinqiao Xie,[3] Manyam Pilla,[3] Debdeep Jena,[1,4] and Huili Grace Xing[1,4,a)]
[1]*School of Electrical and Computer Engineering, Cornell University, Ithaca, New York 14853, USA*
[2]*IQE RF LLC, Somerset, New Jersey 08873, USA*
[3]*Qorvo, Inc., Richardson, Texas 75080, USA*
[4]*Department of Material Science and Engineering, Cornell University, Ithaca, New York 14853, USA*

(Received 28 May 2018; accepted 24 July 2018; published online 7 August 2018)

Thermal activation of buried p-type GaN is investigated in metal-organic chemical vapor deposition-regrown vertical structures, where the buried p-GaN is re-passivated by hydrogen during regrowth. The activation is performed by exposing the buried p-GaN through etched sidewalls and characterized by reverse breakdown measurements on vertical diodes. The effect of the n-type doping level on the activation has been observed. After 725 °C/30 min annealing in a dry air environment, the buried p-GaN with a regrown unintentionally-doped (UID) capping layer is sufficiently activated due to significant Mg-incorporation in the UID layer, allowing for hydrogen up-diffusion. With an additional regrown n^+-GaN capping layer (i.e., in n^+/i/p-n diodes), only lateral diffusion of H out of the exposed mesa sidewall is permitted. A critical lateral dimension between 10 and 20 μm is found for the n^+/i/p-n diodes, under which the buried p-GaN is sufficiently activated. The diodes with activated buried p-GaN achieved up to 1200 V breakdown voltage, indicating that over 28% of the Mg dopants is activated. The study demonstrates the effectiveness of sidewall p-GaN activation in achieving high breakdown voltage pertinent to GaN vertical power devices, while providing guidelines on the required device geometry. *Published by AIP Publishing.*
https://doi.org/10.1063/1.5041879

Due to a unique combination of direct band-gap, high mobility and wide band-gap, GaN is a promising material in both optical and power electronic applications. Based on the vertical p-n diode structure, efficient blue light emission has been achieved[1] and record high Baliga's figure of merit (FOM) has been demonstrated.[2–6] Mg-doped p-type GaN using metal-organic chemical vapor deposition (MOCVD) requires the post-growth activation of the acceptors to release mobile holes.[7,8] It is found that the Mg dopant is passivated due to the incorporation of atomic hydrogen during growth,[9] which exists in H^+ and forms a Mg-H complex.[10–14] Successful activation of p-GaN consists of two steps: breaking the Mg-H bonds and driving away the H^+ out of the material. At elevated temperatures above 700 °C, the Mg-H bonds can be broken and hydrogen can diffuse out from exposed p-GaN surfaces. Improved thermal activation has been achieved by using an O_2 gas mixture[15–17] and hydrogen-storage metals,[18] thanks to augmented hydrogen diffusion by faster exhaustion of the out-diffused hydrogen.

Buried p-GaN structures are essential in tunnel-injection LEDs[19,20] and various vertical power transistors such as HBTs,[21–23] trench-MOSFETs,[24–26] CAVETs,[27–29] LDMOS-like transistors[30,31] and trench-MOSFETs with a regrown channel.[32–36] However, in those device structures, the buried p-type GaN layer can be either passivated during uninterrupted MOCVD growth,[37] or re-passivated by the MOCVD regrowth of a capping layer. The activation of buried p-GaN is much more difficult than that of p-GaN with an exposed top surface mainly due to two reasons: (1) hydrogen has a much higher diffusion barrier[11] and thus a much lower diffusivity in n-type GaN compared with p-type GaN,[12,38] thus it cannot diffuse through the n-type layer on top; (2) the built-in electric field in the top n-p junction prevents H^+ in the buried p-GaN from moving towards the top surface. One possible way of activating the buried p-GaN is by exposing the p-GaN through etched mesa sidewalls and/or via holes.[26,28,29,33,34,39] Effective activation of p-GaN has been tested by reverse breakdown measurement on the body p-n diode.[28] It has also been demonstrated that hydrogen can diffuse laterally out of the mesa sidewalls and activation of the buried p-type layer is confirmed by light emission and reduced turn-on voltage in a tunnel-junction LED structure.[39]

Compared with tunnel-junction LEDs, where insufficient activation of buried p-GaN leads to an effectively "open" circuit, power devices have a more stringent requirement on the activation. Any buried p-GaN region with insufficient activation of the Mg-dopants leads to reduced Gummel number (i.e., the net negative charges in p-GaN), which directly leads to premature punch-through breakdown, i.e., an effective "short" path of the device.[37] In this paper, we investigate the activation of buried p-GaN passivated by hydrogen via etched mesa sidewalls in vertical diode structures using the reverse breakdown measurement as *a sensitive probe pertinent to power electronic applications*. A critical lateral dimension is identified under which sufficient activation of the buried p-GaN is achieved.

The as-grown epitaxial structure [Fig. 1(a)] is of a p-n diode grown by MOCVD on a bulk GaN substrate similar to Refs. 2 and 40, designed to support >1200 V reverse bias. The top 400 nm p-GaN layer has a Mg doping concentration of $1 \times 10^{18}\,cm^{-3}$, capped with a thin p^{++} layer for p-type ohmic contacts, which is activated *in-situ* in the MOCVD

a)Electronic addresses: wl552@cornell.edu and grace.xing@cornell.edu

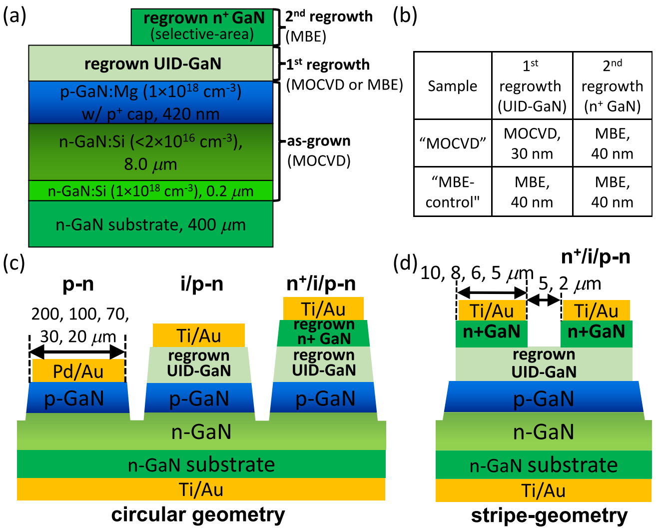

FIG. 1. (a) Schematic layer structure of the as-grown *in-situ* activated p-n diode structure and the two regrown layers. (b) Information on the two regrown layers on the MOCVD and MBE control sample. (c) Schematic cross-sections of three types of circular diodes: p-n, i/p-n and n$^+$/i/p-n diodes fabricated on both samples, with diameters of 200, 100, 70, 30, and 20 μm. (d) Schematic cross-section of the n$^+$/i/p-n diodes with stripe-geometry. The widths of the stripes are designed to be 10, 8, 6, 5 μm. The stripes all have a finger length of 50 μm and are separated by a small i/p-n region (2 or 5 μm) between the two fingers.

reactor. Underneath the p-GaN layer is an 8 μm drift layer with a Si concentration of 1–2 $\times$ 10^{16} cm^{-3}. The net carrier concentration of the drift layer is $\sim$1 $\times$ 10^{16} cm^{-3} as determined from C-V measurements. The resultant contact resistance R_c and Hall measurement data on the p-layer in these as-prepared p-n diodes are among the best in the literature:[2,40] R_c of $\sim$4 $\times$ 10^{-5} Ω·cm^2, hole concentration of $\sim$7% of Mg concentration and hole mobility of 24 cm^2/V·s. These observations confirm that the as-prepared p-layer is well behaved and sufficiently activated to start with.

Two samples with buried p-GaN structures are prepared [Fig. 1(b)]: an MOCVD sample and an MBE (molecular beam epitaxy) control sample. In the MOCVD sample, a buried and H-passivated p-GaN structure is first created by a blanket MOCVD regrowth of a 30-nm unintentionally doped (UID)-GaN capping layer on top of the p-n structure described above. Before loading into the MOCVD chamber, the sample received a 30-min UV-ozone treatment followed by HF cleaning to reduce the residue Si concentration at the surface.[33,34] To ensure full passivation of p-GaN,[9] prior to the UID-GaN regrowth, the MOCVD sample also received a 900 °C/30 min *in-situ* anneal inside the MOCVD growth chamber with NH_3 carrier gas. In the MBE control sample, a buried but un-passivated p-GaN structure is created by a blanket regrowth of a UID-GaN capping layer of similar thickness using MBE at a substrate thermocouple temperature of 800 °C. To investigate the effect of different n-type doping levels in the capping layer, a 40-nm n$^+$-GaN layer is subsequently regrown by MBE on a selected area on both samples. A lift-off process is used with SiO_2 as the hard mask. As a result, 4 types of buried p-GaN structures are compared: MOCVD-i/p-n, MOCVD-n$^+$/i/p-n, MBE-i/p-n, and MBE-n$^+$/i/p-n, with "/" signifying a regrowth interface, while "-" for an interface without growth interruption.

Subsequently, three types of vertical diodes are fabricated on both samples: i/p-n diodes, n$^+$/i/p-n and p-n diodes. All three types of diodes have a circular geometry with the diameter ranging from 200 μm to 20 μm, as shown in Fig. 1(c). In addition, the n$^+$/i/p-n diodes are also available in a stripe-geometry with the stripe width ranging from 10 μm to 5 μm [Fig. 1(d)]. The fabrication steps are as follows. The p-GaN top surface is first exposed by etching away the regrown UID-layer using a Cl-based dry etch for the fabrication of p-n diodes. Then, the device mesa isolation is formed in all device types by dry etch; consequentially, the buried p-GaN is exposed via the mesa sidewalls. After the mesa isolation, a 725 °C/30 min furnace anneal in dry air is performed on the MOCVD sample aiming to activate the buried p-GaN via the mesa sidewall. Finally, the Ti/Au stack and the Pd/Au metal stack are deposited for n-type and p-type ohmic contacts, respectively.

To quickly confirm the re-passivation of p-GaN by hydrogen during the MOCVD regrowth process, diodes on the MOCVD sample are also probed without metallization before and after the activation anneal. Figure 2 shows the leakage current comparison under reverse bias. Both the p-n diodes and the n$^+$/i/-p-n diodes show high leakage current before the activation anneal; no high leakage is observed for the i/p-n diodes, possibly due to the Schottky barrier formed between the probe tip and the sample surface, which limits the leakage current within the bias range. These observations indicate the p-GaN layer being re-passivated inside the MOCVD chamber.

The conductivity of the regrown layers is investigated by the transfer length measurement (TLM). Figure 3(a) shows the gated-TLM I-V curves obtained on the UID-layer of the MOCVD-i/p-n structure at $V_g = 25$ V. The cross-section schematic of the gated-TLM test structure is shown in the inset. The gate dielectric is 30 nm of Al_2O_3 deposited by atomic layer deposition (ALD). The gated-TLM is required since the thin UID-GaN layer should be fully depleted by the p-GaN underneath. At $V_g = 25$ V, the regrown layer shows a high sheet resistivity (R_s) of $\sim$0.1 M$\Omega/\square$, indicating that UID-GaN is strongly compensated, likely due to Mg-diffusion from p-GaN underneath during the MOCVD regrowth.[41] Figure 3(b) shows the TLM I-V

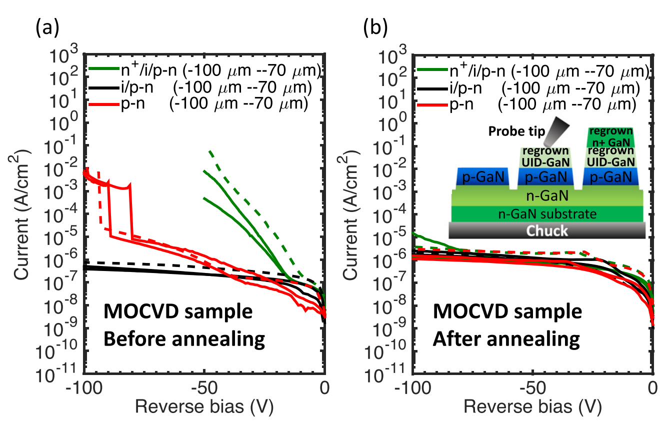

FIG. 2. Reverse I-V measurement of the circular diodes *w/o metal contacts* on the MOCVD sample: (a) before and (b) after the activation annealing at 725 °C for 30 min. The observed high leakage before annealing indicates that the p-GaN layer was re-passivated inside the MOCVD chamber.

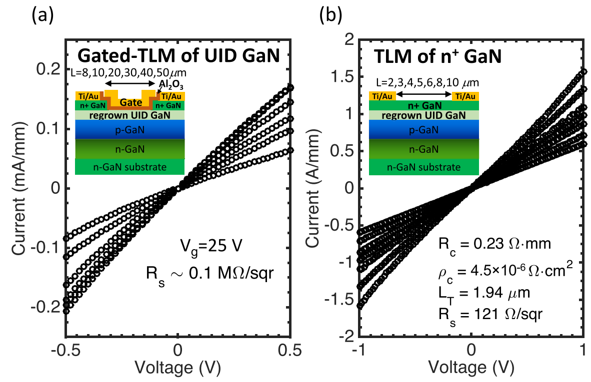

FIG. 3. TLM measurements on the MOCVD sample. (a) Gated-TLM I-V curves of the MOCVD-regrown UID GaN layer, measured at $V_g = 25$ V. (b) TLM I-V curves of the MBE-regrown n^+-GaN layer. Insets show the schematic cross-section of the TLM structures. The gate dielectric in the gated-TLM structure is 30 nm of ALD Al_2O_3.

curves of the MBE-regrown n^+-GaN layer. Excellent contact resistivity (ρ_c) of 4.5×10^{-6} $\Omega \cdot cm^2$ and a reasonably low sheet resistance (R_s) of 121 $\Omega/\square$ are extracted. The R_s value is typical of the MBE-regrown n^+-GaN of such thickness.

The reverse breakdown measurement is performed on the diodes of both samples. Figures 4(a) and 4(b) show the reverse I-V characteristics of the *circular* diodes. On the MOCVD sample [Fig. 4(a)], the p-n and i/p-n diodes show similar behavior: the leakage current level is reasonably low and comparable with the p-n diodes in the MBE control sample [Fig. 4(b)]. The breakdown voltage (BV) is around 1100–1200 V. There is no obvious diode-size dependence in either the leakage current or the BV. The device breakdown is limited by mesa edge breakdown as indicated by the burnt area after breakdown tests. Such behavior is expected due to the absence of edge field management techniques such as field plate. These data suggest a decent reverse blocking capability; thus, sufficient activation of p-GaN in the p-n and i/p-n diodes of all sizes (200–20 μm). With the highest BV of ~1200 V, $\geq$28% of Mg atoms are activated as effective acceptors by calculating the field distribution at punch-through. It is worth emphasizing that 28% is the *lower* bound of activation since the breakdown is limited by edge field crowding but not punch through in these devices.

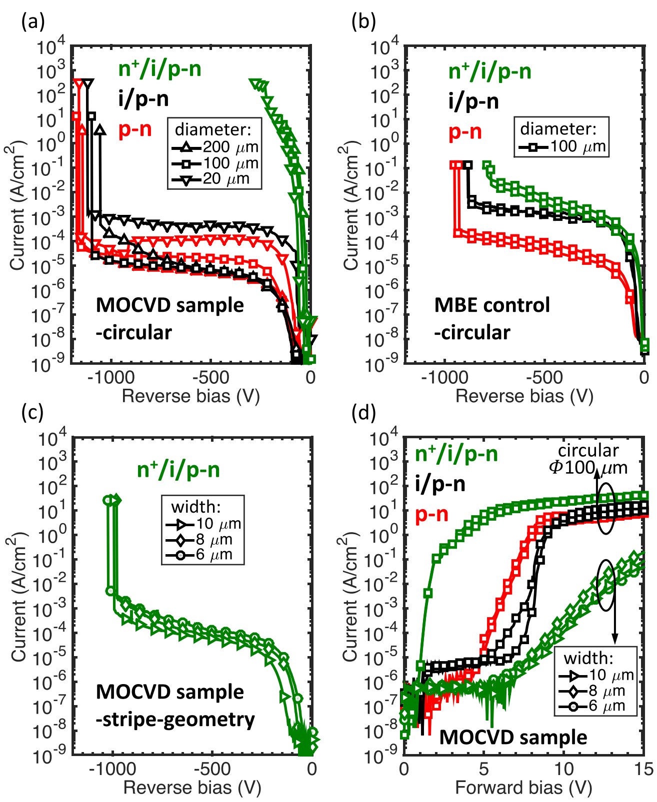

FIG. 4. Reverse and forward I-V characteristics of the three types of diodes. (a) Reverse I-V characteristics of *circular* diodes on the MOCVD sample. (b) Reverse I-V characteristics of *circular* diodes on the MBE control sample. (c) Reverse I-V characteristics of the n^+/i/p-n diodes with *stripe-geometry* on the MOCVD sample. (d) Forward I-V characteristics of the diodes on the MOCVD sample.

On the other hand, the MOCVD-n^+/i/p-n diodes show much higher leakage currents than the p-n and i/p-n diodes. The soft breakdown determined by the measurement compliance is less than 300 V for all device sizes. No clear size dependence is observed. In comparison, the MBE-n^+/i/p-n diodes show much lower leakage currents and much higher BVs, thanks to the absence of hydrogen during MBE regrowth, similar to the report in Ref. 27. These data indicate insufficient activation of the buried p-GaN in the MOCVD-n^+/i/p-n diodes of all diameters from 200 μm to 20 μm.

Activation of p-GaN in the p-n diodes is expected since the top surface of p-GaN is exposed during the activation anneal, allowing hydrogen to diffuse out. On the other hand, activation of buried p-GaN in the MOCVD-i/p-n diodes is not readily expected. As observed from the high reverse leakage current in the circular MOCVD-n^+/i/p-n diodes, the sidewall activation alone is not sufficient for the buried p-GaN in diodes with diameters of 20 μm and above. Consequently, the observed activation of buried p-GaN in the MOCVD-i/p-n diodes does not primarily come from sidewall activation. Instead, the activation should be attributed mostly to diffusion of hydrogen upward toward the top surface. From the gated-TLM measurements and previous studies,[41] substantial Mg incorporation due to Mg-diffusion in the MOCVD-regrown thin UID capping layer is expected. As a result, the UID capping layer behaves like a thin layer of Mg-doped GaN, thus allowing diffusion of hydrogen upward. In the MOCVD-n^+/i/p-n diodes, however, the hydrogen up-diffusion is blocked by the additional n^+-GaN layer. The stark difference in the activation behavior of buried p-GaN in the MOCVD-i/p-n diodes and MOCVD-n^+/i/p-n diodes suggests a strong influence of the net doping in the capping layer on hydrogen diffusion. For circular diodes with sizes down to 20 μm, the sidewall activation alone cannot achieve sufficient activation of the buried p-GaN under the annealing conditions.

For the n^+/i/p-n diodes with a lateral dimension of <20 μm, the *stripe-geometry* with widths of 10, 8, 6, and 5 μm are designed instead of the circular geometry for easy probing. As shown in Fig. 1(d), each diode consists of two 50 μm-long fingers separated by a narrow i/p-n region in between (2–5 μm). Figure 4(c) shows the reverse breakdown results of the stripe-shaped MOCVD-n^+/i/p-n diodes: all measured diodes show low leakage currents and decent BV values, comparable to the activated circular p-n diodes. No clear dependence on the stripe width is observed. Figure 5

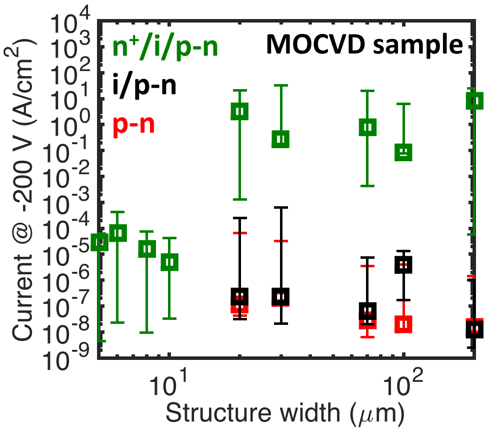

FIG. 5. Reverse leakage current at -200 V vs. structure width for three types of diodes in the MOCVD sample. The error bars are generated based on the measurements of at least 3 devices with identical geometries. The sharp change in leakage near a width of 10–20 μm of the n^+/i/p-n diodes suggests that the buried p-GaN is sufficiently activated in small diodes ($\leq$10 μm) but not in large diodes ($\geq$20 μm).

shows the reverse leakage current at -200 V for all types of diodes on the MOCVD sample with respect to the lateral structure width. At least 3 devices are measured for each diode type and size. The error bars are generated based on the scattering in measured data. A dramatic change in the leakage current for the MOCVD-n^+/i/p-n diodes is observed at $\sim$10–20 μm. These data indicate sufficient activation of the buried p-GaN, and thus a lateral hydrogen diffusion length of $>$5 μm (half of the stripe width) under the annealing conditions is used in this work. The observed activation should be attributed to the lateral diffusion of hydrogen out of the etched mesa sidewall as well as the exposed UID-GaN surface between fingers.

The forward I-V characteristics of the diodes are also measured on the MOCVD samples before the reverse breakdown measurements, as shown in Fig. 4(d). The i/p-n diodes and p-n diodes behave similarly, which supports the argument that the i-layer is converted to p-type due to Mg diffusion. The higher-than-ideal turn-on voltage and the low on-current are due to the poor ohmic contact on the p-layer. The large circular n^+/i/p-n diodes show high leakage current at low bias, while the ones with stripe-geometry and smaller width ($\leq$10 μm) have much lower leakage current, which are consistent with the reverse I-V characteristics.

From the above observations, it can be concluded that the critical lateral dimension of a buried p-GaN layer is between 10 and 20 μm to achieve "effective" activation ($\geq$28% in the structure and annealing conditions used in this work) via exposed p-GaN surfaces, corresponding to a Mg activation length or a H diffusion length of 5–10 μm. This value is about 10$\times$ smaller than the reported Mg activation length of $\sim$85 μm in tunnel-junction LEDs,[39] and the origins of this difference are worthy of further investigations. Presently, we speculate that the much higher Mg concentration in p-GaN used in Ref. 39 may lead to different activation behavior. More importantly, the reverse breakdown measurement is a much *stricter* test of the acceptor activation of buried p-GaN than light emission. Any insufficient activation of buried p-GaN leads to drastically higher leakage current due to premature punch-through.

In order to extend the Mg activation length further into the center of a device, a longer activation time or a higher temperature may be required. At the initial stage of the buried p-GaN activation via mesa sidewall, the concentration gradient of hydrogen is the highest near the sidewall surface. With the activation of p-GaN near the exposed surface, an electric field is established pointing from the un-activated region toward the activated p-GaN, which also promotes the out-drift of hydrogen by exerting an electric force on the H^+ toward the surface. As the activation length increases laterally, both the concentration gradient and the built-in electric field reduce, and thus the activation activity slows down. If the electric field is neglected, the hydrogen profile determined by a lateral diffusion process could be approximately expressed using Fick's law in one-dimension

$$N_{H^+}(x,t) = N_0\,\mathrm{erf}\left(\frac{x}{2\sqrt{Dt}}\right), \tag{1}$$

where x is the distance from the mesa edge, D is the diffusivity of hydrogen, which increases exponentially with increasing temperature, erf is the error function, and N_0 is the initial hydrogen concentration. As suggested by this expression, the characteristic diffusion length is $2\sqrt{Dt}$. Thus, the buried p-GaN should eventually be all activated at sufficiently long annealing times and high annealing temperatures regardless of the dimension. But, it is not practical, given the high thermal budget required and possible material degradation under long-duration high-temperature annealing. The critical lateral dimension found in this study under typical annealing conditions provides valuable insights into the design of devices that incorporate buried p-GaN structures, especially for those used in power electronic applications.

From Eq. (1), the diffusivity of hydrogen at 725 °C in p-GaN can also be estimated. The hydrogen diffusion length is taken to be 5–10 μm, over which the hydrogen concentration is assumed to decrease from $\sim$80% to 0, similar to the criterion used in Ref. 39. The diffusivity D is calculated to be 0.4–1.7 $\times 10^{-10}$ cm^2/s. This value is similar to the estimated hydrogen diffusivity of $\sim 0.4 \times 10^{-10}$ cm^2/s at $\sim$700 °C in Ref. 8, where the hydrogen diffuses vertically out of the p-GaN surface.

In conclusion, the sidewall activation of buried p-GaN in MOCVD-regrown vertical structures is investigated and the effectiveness of the activation is probed by reverse breakdown measurements. The buried p-GaN with a MOCVD-regrown UID layer on top can be activated from the top surface due to the Mg incorporation in the regrown UID film. In the n^+/i/p-n diodes, hydrogen up-diffusion is blocked by the additional n^+-GaN layer but sidewall activation is found to be an effective alternative by utilizing lateral diffusion of hydrogen out of the p-GaN. A critical lateral dimension of 10–20 μm is found for the buried p-GaN structure, under which sufficient sidewall activation of the p-GaN (the lower bound estimate is 28% activation of Mg) is obtained under a 725 °C/30 min anneal in dry air. The diffusivity of hydrogen in p-GaN at 725 °C is estimated to be $\sim 1 \times 10^{-10}$ cm^2/s. This study confirms that high breakdown voltage can be achieved by sidewall activation of p-GaN in power electronic devices utilizing MOCVD-grown/regrown buried p-GaN structures, while providing guidelines on design of the required device geometries.

This work was supported in part by the ARPA-E SWITCHES Program (No. DE-AR0000454) monitored by Tim Heidel and Isik Kizilyalli, in part by AFOSR under Grant No. FA9550-17-1-0048 monitored by Ken Goretta, and carried out at the Cornell Nanoscale Science and Technology Facilities (CNF) sponsored by the NSF NNCI Program (No. ECCS-1542081).

[1]S. Nakamura, T. Mukai, and M. Senoh, Appl. Phys. Lett. **64**, 1687 (1994).
[2]Z. Hu, K. Nomoto, B. Song, M. Zhu, M. Qi, M. Pan, X. Gao, V. Protasenko, D. Jena, and H. G. Xing, Appl. Phys. Lett. **107**, 243501 (2015).
[3]K. Nomoto, Z. Hu, B. Song, M. Zhu, M. Qi, R. Yan, V. Protasenko, E. Imhoff, J. Kuo, N. Kaneda, T. Mishima, T. Nakamura, D. Jena, and H. G. Xing, in *IEEE IEDM* (2015), p. 9.7.
[4]H. Ohta, N. Kaneda, F. Horikiri, Y. Narita, T. Yoshida, T. Mishima, and T. Nakamura, IEEE Electron Device Lett. **36**, 1180 (2015).
[5]A. M. Armstrong, A. A. Allerman, A. J. Fischer, M. P. King, M. S. van Heukelom, M. W. Moseley, R. J. Kaplar, J. J. Wierer, M. H. Crawford, and J. R. Dickerson, Electron. Lett. **52**, 1170 (2016).
[6]Z. Hu, K. Nomoto, M. Qi, W. Li, M. Zhu, X. Gao, D. Jena, and H. G. Xing, IEEE Electron Device Lett. **38**, 1071 (2017).
[7]H. Amano, M. Kito, K. Hiramatsu, and I. Akasaki, Jpn. J. Appl. Phys. **28**, L2112 (1989).
[8]S. Nakamura, T. Mukai, M. Senoh, and N. Iwasa, Jpn. J. Appl. Phys. **31**, L139 (1992).
[9]S. Nakamura, N. Iwasa, M. Senoh, and T. Mukai, Jpn. J. Appl. Phys. **31**, 1258 (1992).
[10]J. Neugebauer and C. G. Van de Walle, Phys. Rev. Lett. **75**, 4452 (1995).
[11]J. Neugebauer and C. G. Van de Walle, Appl. Phys. Lett. **68**, 1829 (1996).
[12]W. Götz, N. M. Johnson, J. Walker, D. P. Bour, H. Amano, and I. Akasaki, Appl. Phys. Lett. **67**, 2666 (1995).
[13]W. Götz, N. M. Johnson, D. P. Bour, M. McCluskey, and E. E. Haller, Appl. Phys. Lett. **69**, 3725 (1996).
[14]Y. Okamoto, M. Saito, and A. Oshiyama, Jpn. J. Appl. Phys. **35**, L807 (1996).
[15]B. A. Hull, S. E. Mohney, H. S. Venugopalan, and J. C. Ramer, Appl. Phys. Lett. **76**, 2271 (2000).
[16]T. C. Wen, S. C. Lee, W. I. Lee, T. Y. Chen, S. H. Chan, and J. S. Tsang, Jpn. J. Appl. Phys. **40**, L495 (2001).
[17]C. H. Kuo, S. J. Chang, Y. K. Su, L. W. Wu, J. K. Sheu, C. H. Chen, and G. C. Chi, Jpn. J. Appl. Phys. **41**, L112 (2002).
[18]I. Waki, H. Fujioka, M. Oshima, H. Miki, and M. Okuyama, J. Appl. Phys. **90**, 6500 (2001).
[19]T. Takeuchi, G. Hasnain, S. Corzine, M. Hueschen, R. P. Schneider, Jr., C. Kocot, M. Blomqvist, Y. L. Chang, D. Lefforge, M. R. Krames, and L. W. Cook, Jpn. J. Appl. Phys. **40**, L861 (2001).
[20]S. R. Jeon, Y. H. Song, H. J. Jang, G. M. Yang, S. W. Hwang, and S. J. Son, Appl. Phys. Lett. **78**, 3265 (2001).
[21]L. S. McCarthy, P. Kozodoy, M. J. W. Rodwell, S. P. DenBaars, and U. K. Mishra, IEEE Electron Device Lett. **20**, 277 (1999).
[22]L. S. McCarthy, I. P. Smorchkova, H. Xing, P. Kozodoy, P. Fini, J. Limb, D. L. Pulfrey, J. S. Speck, M. J. Rodwell, S. P. DenBaars, and U. K. Mishra, IEEE Trans. Electron Devices **48**, 543 (2001).
[23]H. Xing, P. M. Chavarkar, S. Keller, S. P. DenBaars, and U. K. Mishra, IEEE Electron Device Lett. **24**, 141 (2003).
[24]T. Oka, T. Ina, Y. Ueno, and J. Nishii, Appl. Phys. Express **8**, 054101 (2015).
[25]R. Li, Y. Cao, M. Chen, and R. Chu, IEEE Electron Device Lett. **37**, 1466 (2016).
[26]C. Liu, R. A. Khadar, and E. Matioli, IEEE Electron Device Lett. **39**, 71 (2018).
[27]R. Yeluri, J. Lu, C. A. Hurni, D. A. Browne, S. Chowdhury, S. Keller, J. S. Speck, and U. K. Mishra, Appl. Phys. Lett. **106**, 183502 (2015).
[28]D. Ji, M. A. Laurent, A. Agarwal, W. Li, S. Mandal, S. Keller, and S. Chowdhury, IEEE Trans. Electron Devices **64**, 805 (2017).
[29]D. Ji, A. Agarwal, H. Li, W. Li, S. Keller, and S. Chowdhury, IEEE Electron Device Lett. **39**, 863 (2018).
[30]H. Nie, Q. Diduck, B. Alvarez, A. P. Edwards, B. M. Kayes, M. Zhang, G. Ye, T. Prunty, D. Bour, and I. C. Kizilyalli, IEEE Electron Device Lett. **35**, 939 (2014).
[31]H. G. Xing, B. Song, M. Zhu, Z. Hu, M. Qi, K. Nomoto, and D. Jena, in *Proceedings 73rd Annual Device Research Conference (DRC)* (2015), p. 51.
[32]D. Shibata, R. Kajitani, M. Ogawa, K. Tanaka, S. Tamura, T. Hatsuda, M. Ishida, and T. Ueda, in *IEEE IEDM* (2016), p. 10.1.
[33]C. Gupta, C. Lund, S. H. Chan, A. Agarwal, J. Liu, Y. Enatsu, S. Keller, and U. K. Mishra, IEEE Electron Device Lett. **38**, 353 (2017).
[34]D. Ji, C. Gupta, S. H. Chan, A. Agarwal, W. Li, S. Keller, U. K. Mishra, and S. Chowdhury, in *IEEE IEDM* (2017), p. 9.4.
[35]W. Li, K. Nomoto, K. Lee, S. M. Islam, Z. Hu, M. Zhu, X. Gao, M. Pilla, D. Jena, and H. G. Xing, in *Proceedings of the 75th Annual Device Research Conference (DRC)* (2017), p. 1.
[36]W. Li, K. Nomoto, K. Lee, S. M. Islam, Z. Hu, M. Zhu, X. Gao, M. Pilla, D. Jena, and H. G. Xing, IEEE Trans. Electron Devices **65**, 2558 (2018).
[37]W. Li, M. Zhu, K. Nomoto, Z. Hu, X. Gao, M. Pilla, D. Jena, and H. G. Xing, in 2018 *IEEE 30th International Symposium on Power Semiconductor Devices and ICs (ISPSD)* (2018), p. 228.
[38]A. Y. Polyakov, N. B. Smirnov, S. J. Pearton, F. Ren, B. Theys, F. Jomard, Z. Teukam, V. A. Dmitriev, A. E. Nikolaev, A. S. Usikov, and I. P. Nikitina, Appl. Phys. Lett. **79**, 1834 (2001).
[39]Y. Kuwano, M. Kaga, T. Morita, K. Yamashita, K. Yagi, M. Iwaya, T. Takeuchi, S. Kamiyama, and I. Akasaki, Jpn. J. Appl. Phys. **52**, 08JK12 (2013).
[40]W. Li, K. Nomoto, M. Pilla, M. Pan, X. Gao, D. Jena, and H. G. Xing, IEEE Trans. Electron Devices **64**, 1635 (2017).
[41]H. Xing, D. S. Green, H. Yu, T. Mates, P. Kozodoy, S. Keller, S. P. DenBaars, and U. K. Mishra, Jpn. J. Appl. Phys. **42**, 50 (2003).